

# Extremely broadband calibrated bolometers and microbolometer arrays for Earth radiation budget measurements

M. Stephens<sup>\*a</sup>, C. S. Yung<sup>a</sup>, N. A. Tomlin<sup>a</sup>, D. Harber<sup>b</sup>, C. Straatsma<sup>b</sup>, A. Dan<sup>a</sup>, E. Freire Antunes<sup>a</sup>, P. Pilewski<sup>b</sup>, O. Coddington<sup>b</sup>, J. H. Lehman<sup>a</sup>

<sup>a</sup>National Institute of Standards and Technology, Applied Physics Division, 325 Broadway, Boulder, CO 80305; <sup>b</sup>Laboratory for Atmospheric and Space Physics, University of Colorado Boulder, Boulder, CO 80309

## ABSTRACT

The Earth radiation budget, a 40-year data record of the balance between solar radiation reaching the Earth and the amount reflected, and emitted from the Earth, is a key climate record for determining whether the Earth is warming or cooling. The need for accurate and cost-effective space-based measurements is driving the technology development of broadband bolometers and linear microbolometer arrays. We describe the performance of microfabricated bolometers and 1 x 32 linear microbolometer arrays developed for this purpose. To accurately measure the total outgoing radiation from 0.3  $\mu\text{m}$  to over 100  $\mu\text{m}$ , consisting of reflected shortwave solar radiation and emitted longwave thermal radiation, a vertically aligned carbon nanotube thermal absorber is incorporated with an electrical substitution heater that provides on-board calibration capabilities. A silicon nitride heat link is used to optimize response time while minimizing noise and the inequivalence between thermal and optical heating. The devices operate at room temperature with noise floors at  $n\text{W}/\sqrt{\text{Hz}}$  or lower at the measurement frequency of 7 Hz. Response times below 10 ms have been demonstrated in closed-loop operation using the electrical heater. Thin film Pt thermistors measure the change in microbolometer temperature. The deposition of the thin film thermistors has been optimized to maximize the temperature coefficient of resistance, which is key to meeting the demanding signal-to-noise requirement of this application.

**Keywords:** Radiometer, bolometer, carbon nanotubes, Earth radiation budget, microbolometer array, infrared detector

## 1. INTRODUCTION

The Earth receives energy from the sun and loses energy to space by either reflecting the incident solar radiation or by absorbing it, warming, and then emitting the energy through thermal radiation. The top-of-atmosphere (TOA) balance between the solar energy received – the total solar irradiance (TSI) - and the total energy lost - outgoing radiation - is referred to as the Earth Radiation Budget (ERB). The ERB is a fundamental radiative force on the Earth's climate system and is an essential climate variable (ECV).<sup>1</sup> The ERB is measured via satellite and requires radiometric accuracy of 0.5% over wavelengths from 0.3  $\mu\text{m}$  to 100  $\mu\text{m}$ .<sup>2</sup> The existing 40-year TSI data record is constructed from direct solar irradiance measurements made with a series of successively more accurate radiometers.<sup>3</sup> Measurements of outgoing radiation have been provided by the NASA Clouds and Earth's Radiant Energy System (CERES) project since 1997<sup>4</sup> using broadband scanning radiometers. However, these instruments are large and expensive. Maintaining data continuity for the ERB is important for understanding long-term changes in the Earth's climate. By developing smaller, but more accurate radiometers, the cost of future continuity missions can be reduced. Furthermore, by developing radiometer arrays, spatially resolved measurements of the ERB can be made. This enables study of the impact of cloud-radiative forcing on the ERB at 1 km spatial resolutions. Here we demonstrate a 1x32 array of broadband microfabricated bolometers with electrical substitution for ERB measurements.

Microfabricated bolometers and microbolometer arrays with high, broadband absorptivity provided by vertically aligned carbon nanotubes (VACNTs) and electrical substitution heaters provide several advantages over traditional radiometers. The VACNTs can provide high absorptance (reflectivity below 1000 ppm out to 2  $\mu\text{m}$ <sup>5</sup> and below 1% out to 100  $\mu\text{m}$ ). With such a low reflectivity, an additional conical absorber to enhance absorption is no longer necessary, and the bolometer can be fabricated with a planar geometry. As a result, the size and mass can be reduced to create a broadband

---

\* [michelle.stephens@nist.gov](mailto:michelle.stephens@nist.gov); phone 1 303 497-3742; nist.gov

highly absorbing bolometer array with a short time constant and high sensitivity at room temperature. The planar geometry and small size enabled by the VACNTs are compatible with lithographic fabrication. This extremely precise process enables the design and fabrication of carefully tuned devices that can have a well-controlled thermal conductance and very low optical and electrical inequivalence (i.e., the mismatch between the bolometer response to power deposited by using an optical source and by using an electrical source). It also enables including a heater and therefore electrical substitution calibration on each pixel. This has two benefits. First, the pixel can be operated closed loop, which speeds up the response, and second, careful monitoring of the electrical power to the heater can be used to calibrate the array and monitor degradation of the instrument.

While using the VACNTs as a broadband absorber enables miniaturization for broadband applications, their use also leads to special considerations. The VACNT growth process used at NIST produces extremely black, broadband VACNT forests. Once grown, these VACNTs can be sprayed with compressed air, but they are not robust to liquids or physical touch. As a result, VACNT growth is the last step in device fabrication. The NIST process for VACNT growth is typically at 750 °C to 850 °C, while flowing Ar, H<sub>2</sub>, and C<sub>2</sub>H<sub>4</sub> at a total pressure of 2666.5 Pa (20 Torr), and an applied microwave power of 900 W.<sup>6</sup> Exposing a microfabricated device to such a harsh environment can cause changes in material properties and create mechanical stresses in thin film metal layers used for wiring, heaters, and thermistors that, without careful attention to design and fabrication that uses materials and process steps that are compatible with high temperatures, can adversely affect the performance of the device.<sup>6</sup> Other considerations that must be taken into account in the design and fabrication are that VACNTs grow differently on different surfaces, passivation layers may be required to prevent shorting between layers caused by the environment,<sup>6</sup> and while longer (greater than ~ 40 μm) VACNTs have lower reflectivity, they also have higher thermal mass and slow down the response of the detector.

Single element, microfabricated VACNT bolometers are on CubeSats in low Earth orbit as part of the Compact Spectral Irradiance Monitor (CSIM)<sup>7</sup>, the Compact Total Irradiance Monitor (CTIM)<sup>8</sup>, and the Radiometer Assessment using Vertically Aligned Nanotubes (RAVAN) mission included a VACNT radiometer.<sup>9</sup> This paper describes the fabrication and performance of 1 x 32 linear microbolometer arrays under development for ERB measurements.<sup>10</sup>

## 2. MICROBOLOMETER ARRAY DESIGN AND PERFORMANCE

A bolometer measures optical power by absorbing the incident power, converting it to heat, and measuring the temperature change of the detector. The magnitude and rise time of the temperature change are determined by the absorptance of the bolometer, the size and heat capacity of the absorber, and the design of a weak thermal link between the absorber and the surrounding environment. A bolometer calibrated by electrical substitution incorporates a heater of known resistance on the absorber. Measurement of the electrical power needed to raise the temperature of the bolometer when optical power is *not* incident to the same temperature measured when optical power *is* incident on the absorber determines the electrical power that is equivalent to the optical power. This in turn provides a calibrated value for optical power traceable to the SI (Figure 1).<sup>11</sup>

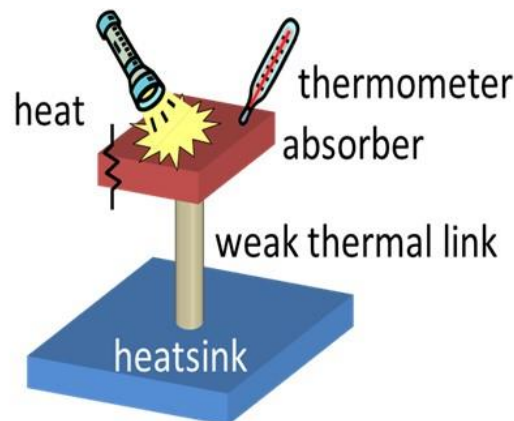


Figure 1. The basic components of a bolometer calibrated with electrical substitution include an absorber, thermometer, weak thermal link, heatsink, and resistive heater.

For the best signal-to-noise (SNR) the absorptance should be high (i.e., low reflectance) over the wavelength of the incident light, and the temperature sensor should have a high sensitivity to temperature change and exhibit low  $1/f$  noise. To image clouds from orbit with a spatial resolution of around 1 km, the response time should be on the order of 10 ms or less. Traditional microbolometers use a thermistor as both the temperature sensor and absorber. To maximize the absorption within the thermistor, they use reflective coatings to create an optical cavity around the thermistor. This allows light that is initially transmitted through the thermistor to be reflected back to the thermistor, which results in higher optical absorption. However, it limits the absorption to a relatively narrow band around 8  $\mu\text{m}$  to 15  $\mu\text{m}$  because of the design of the reflective coatings. Vertically aligned carbon nanotubes are an excellent choice as an alternate absorber because of their extremely low reflectance at wavelengths over the whole 0.3  $\mu\text{m}$  – 100  $\mu\text{m}$  science band. However, this means a separate thermistor must be used.

The CSIM and CTIM bolometers use surface mount commercial thermistors epoxied to the bolometer after VACNT growth. However, for an array, the smaller pixel size ( $\sim 100 \mu\text{m}$  square), fast response time required, and number of elements ( $1 \times 32$ ) desired for ERB measurements prohibit the use of bonded commercial thermistors. Rather, the thermistors need to be thin-film thermistors. Commercial microbolometer arrays typically use vanadium oxide ( $\text{VO}_x$ ) thin films for temperature measurement because it has a high temperature coefficient of resistance (TCR) that can exceed 3 %/ $^\circ\text{C}$ .<sup>12</sup> While  $\text{VO}_x$  survives VACNT growth, good noise and response performance after growth proved difficult to achieve, and the resistance was also often higher than desired for the application. Instead, we have chosen to develop processes utilizing Pt thin film thermistors. Even though the TCR of a thin film Pt thermistor is a factor of ten lower (0.308 %/ $^\circ\text{C}$ )<sup>13</sup> the greatly reduced  $1/f$  noise and the stability through the VACNT growth process makes it a better choice. Reference 12 discusses the optimization of the Pt thin film resistors for VACNT bolometers in greater detail. VACNTs themselves can be used as thermistors<sup>10</sup>, but for this application they are not optimal, as they tend to have higher  $1/f$  noise and increase the thermal mass (and therefore lower the response time) of the bolometer pixel.

To speed up the performance and to provide the calibration capabilities discussed in the next section, the Pt thermistor is also used as a heater. Readout of the optical power incident on each pixel is accomplished by placing each pixel in a resistance bridge and using pulse-width modulation (PWM) of a stable voltage reference (e.g., LTZ1000) to deliver electrical heater power to the heater/thermistor. As the scene imaged by each pixel changes, the electrical power can be adjusted to maintain each pixel at a constant temperature. This serves two purposes. First, the closed loop operation speeds up the response of the pixel to below 10 ms, which has been demonstrated previously.<sup>10</sup> Second, by using the precision voltage reference and in-series resistor, the electrical power needed to compensate for changing optical power can provide calibration and aging information about the pixel.

Figure 2 shows images of the fabricated microbolometer pixels. Each pixel is  $124 \mu\text{m} \times 124 \mu\text{m}$ . The four heat links are  $\text{SiN}_x$  legs, 100  $\mu\text{m}$  long  $\times$  8  $\mu\text{m}$  wide  $\times$  0.5  $\mu\text{m}$  thick. The center-to-center spacing of the pixels is 160  $\mu\text{m}$ . Figure 3 shows a complete  $1 \times 32$ -pixel linear array.

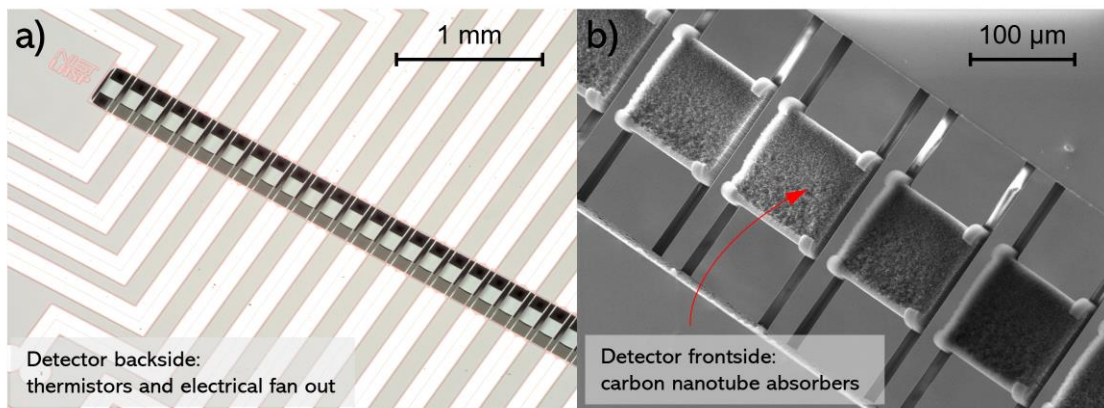


Figure 2 Images of microbolometer pixels. In a) a 32-element linear array is shown. Each pixel is suspended with four thermal links. Electrical traces to the Pt heater/thermistor (not visible in this image) are routed up the thermal link. In b) the opposite side of the pixels are seen with the VACNT absorbers are shown

The Si chip that contains the fabricated  $1 \times 32$  linear array includes expansion traces that allow the chip to be mounted in a chip carrier with the electrical connections wire bonded (Figure 3).

Figure 4 shows the measured noise performance of the microbolometer array at two different values of the electrical replacement power. The noise decreases with increased electrical power (i.e., increased bias current). With  $10 \mu\text{W}$  of replacement power, the pixel experiences a  $5^\circ\text{C}$  rise in temperature and has  $100 \text{ pW}/\sqrt{\text{Hz}}$  noise in the detection band. With  $88 \mu\text{W}$  of replacement power the pixel experiences a  $45^\circ\text{C}$  rise in temperature and has  $40 \text{ pW}/\sqrt{\text{Hz}}$  noise in the detection band. A  $45^\circ\text{C}$  temperature rise is a reasonable operating point, and this is sufficient to meet the sensitivity requirements for cloud radiation measurements with a  $1 \text{ km}$  spatial resolution for the ERB using a telescope that is small enough to allow an instrument package on a 12U CubeSat. This will be discussed in greater detail in the next section.

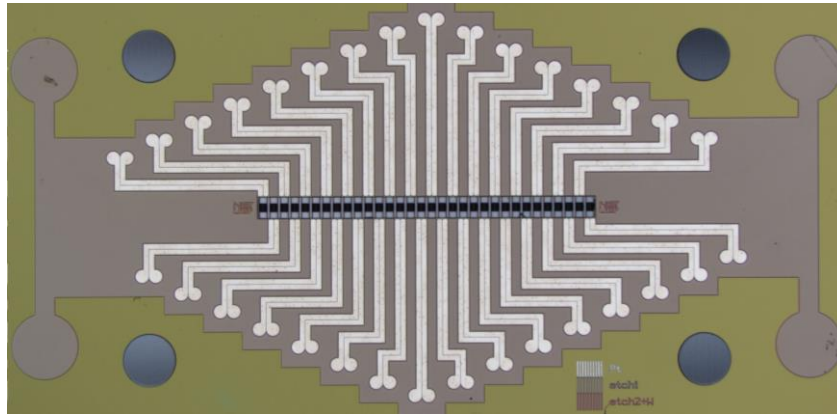


Figure 3.  $1 \times 32$  microbolometer array chip. The 32 pixels are in the center of the image. Electrical traces leading to the thermistor/heater can be seen leading from the top and bottom of the array. These traces will be wire bonded to a chip carrier as a final packaging step.

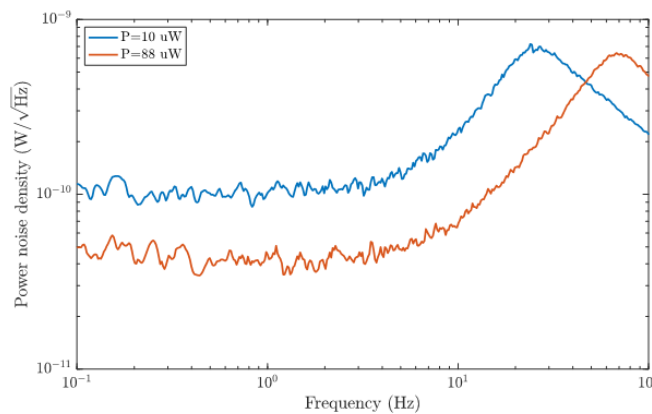


Figure 4. The noise floor in the 7 Hz detection band is  $40 - 100 \text{ pW}/\sqrt{\text{Hz}}$ , depending on the electrical replacement power.

### 3. APPLICATION TO EARTH RADIATION BUDGET MEASUREMENTS

The Earth's radiative imbalance, the difference between total incoming and total outgoing energy at TOA, is estimated to be approximately  $0.6 \text{ W}/\text{m}^2$ ,<sup>14</sup> and the uncertainty requirements for measuring the top-of-atmosphere components of Earth's radiative energy budget can be established by the need to resolve it. First, to maintain continuity with the 22-year record from the CERES mission, accuracy requirements for the outgoing reflected solar and emitted terrestrial radiance

are on the order of 0.5%.<sup>2</sup> The anticipated accuracy is discussed below. In addition, to image with a 1 km spatial resolution over the 0.3  $\mu\text{m}$  to 100  $\mu\text{m}$  wavelength band and extract information on the effects of radiative cloud forcing, we have set a goal of  $< 0.1 \text{ W/m}^2\text{-sr}$  radiometric precision.<sup>15</sup> With the measured pixel noise performance, an approximately 30-mm aperture telescope is sufficient to meet the radiometric precision requirements and is compatible with a total instrument package on a 12U CubeSat.

Absolute accuracy requires good calibration and stability on-orbit. Existing instruments are calibrated on the ground but then subjected to severe launch and space environments. On-orbit calibration is typically achieved with an on-orbit reference such as a blackbody, lamp, or reference material and by ground verification. On-orbit references increase payload mass and power requirements and are degraded by the space environment. Comparison with ground-based measurements adds uncertainty through correction for atmospheric effects. This technology incorporates electrical substitution calibration to augment the traditional calibration methods. By comparing the temperature rise of the bolometer when illuminated to the temperature rise when a known current is injected into the heater of known resistance, a calibrated irradiance is measured. Commercially available voltage references and precision resistors have both the accuracy, the stability, and the space heritage to provide a well-calibrated stable on-orbit current.<sup>7,8</sup> This information can be used as an additional monitor of the overall degradation of the system (detector and telescope) when viewing vicarious ground calibration sites or in duty-cycle comparisons of on-orbit observations from an often-used instrument relative to one that has been less exposed.

#### 4. CONCLUSIONS

We have described a  $1 \times 32$  linear microbolometer array capable of operating over the full 0.3  $\mu\text{m}$  to 100  $\mu\text{m}$  wavelength range of interest for the ERB by using VACNTs as the optical absorber. The array is designed so that it can be used to image clouds with a spatial resolution of 1 km and obtain information about the cloud radiative forcing impact on the ERB. The pixels are  $124 \mu\text{m} \times 124 \mu\text{m}$  with a noise floor of 40 - 100  $\text{pW}/\sqrt{\text{Hz}}$  in the 7 Hz detection band required for 1 km spatial resolution from low Earth orbit. Each pixel can be operated closed loop via an electrical substitution technique. This provides both on-orbit monitoring of calibration drift and a response time of less than 10 ms. An ESR microbolometer array with a VACNT absorber improves the measurements by enabling a lower mass, lower power, spectrally broad instrument with absolute on-orbit calibration. Although our development has focused on ERB, the combination of broadband spectral response and integrated calibration capability makes this single technology applicable across a broad range of scientific measurements such as water vapor measurements or solar spectral irradiance imaging.

#### ACKNOWLEDGEMENTS

This work was funded in part by the NASA Earth Science Technology Office (ESTO) Advanced Component Technology (ACT) program and the ESTO Instrument Incubator Program (IIP).

This manuscript is a contribution of the United States Government and is not subject to copyright. Certain commercial equipment, instruments, or materials are identified in this paper to specify the experimental procedure adequately. Such identification is not intended to imply recommendation or endorsement by the National Institute of Standards and Technology, nor is it intended to imply that the materials or equipment identified are necessarily the best available for the purpose.

#### REFERENCES

- [1] "Systematic observation requirements for satellite-based products for climate, 2011 update," WMO GCOS Rep. 154, 30-31 (2011).
- [2] Barki, A. et al., Report of the Earth Venture Continuity Radiation Budget Science Working Group: "Recommended Measurement and Instrument Characteristics for an Earth Venture Continuity Earth Radiation Budget Instrument, NASA, v (2018). <[https://essp.larc.nasa.gov/EVC-1/pdf\\_files/ERB\\_SWG\\_Rept\\_FINAL.pdf](https://essp.larc.nasa.gov/EVC-1/pdf_files/ERB_SWG_Rept_FINAL.pdf) >

- [3] Kopp, G. et al., "Total solar irradiance data record accuracy and consistency improvements," *Metrologia* 49, S29-S33 (2012).
- [4] Loeb, N.G. et al., "CERES Top-of-Atmosphere Earth Radiation Budget Climate Data Record: Accounting for in-Orbit Changes in Instrument Calibration," *Remote Sens.* 8, 182 (2016).
- [5] Lehman, J. et al., "Carbon nanotube-based black coatings," *Applied Physics Reviews* 5, 011103 (2018).
- [6] Tomlin, N.A. et al. " Overview of microfabricated bolometers with vertically aligned carbon nanotube absorbers," *AIP Advances* 10, 0550010 (2020).
- [7] Richard, E. et al., "Compact spectral irradiance monitor flight demonstration mission," *Proc. SPIE* 11131, 111310D5 (2019).
- [8] Harber, D. et al., "Compact total irradiance monitor flight demonstration," *Proc. SPIE* 11131, 111310D1 (2019).
- [9] Swartz, W.H. et al., "The RAVAN CubeSat mission: Advancing technologies for climate observation," 015 *IEEE International Geoscience and Remote Sensing Symposium (IGARSS)*, 5300 (2015)
- [10] Yung, C.S. et al., "BABAR: black array of broadband absolute radiometers for far infrared sensing," *Proc. SPIE* 10980, *Image Sensing Technologies: Materials, Devices, Systems, and Applications VI*, 109800F (2019).
- [11] Martin, J.E, Fox, N.P., and Key, P.J., "A Cryogenic Radiometer for Absolute Radiometric Measurements," *Metrologia* 21, 147 (1985).
- [12] Rogalski, A., [*Infrared and Terahertz Detectors, Third Edition*], CRC Press, Boca Raton, London & New York, 156 (2022).
- [13] Dan, A., Antunes, E., Yung, C., Tomlin, N., Stephens, M., Lehman, J., "Effects of annealing conditions on temperature coefficient of resistance of Pt thin-film thermistors," *International Conference on Metallurgical Coatings and Thin Films*, San Diego, CA, USA (2022).
- [14] National Research Council, *Report on Evaluating NOAA's plan to Mitigate the Loss of Total Solar Irradiance Measurements from Space*, Washington, DC: The National Academies Press, 2013.
- [15] Coddington, O. and Straatsma, C., *Laboratory for Atmospheric and Space Physics, University of Colorado Boulder*, private communication, May 25, 2022.